ISSN 1063-4576, Journal of Superhard Materials, 2022, Vol. 44, No. 6, pp. 413–420. © Allerton Press, Inc., 2022.
Ukrainian Text © The Author(s), 2022, published in Nadtverdi Materialy, 2022, Vol. 44, No. 6, pp. 44–52.

SYNTHESIS, STRUCTURE, AND PROPERTIES

Influence of the Bias Potential and Working Gas Pressure on the Properties of the TiSiN/NbN Ion Plasma Multilayer Coating

D. V. Horokh[a], O. V. Maksakova[a], S. A. Klymenko[b, *], S. V. Lytovchenko[a], V. M. Beresnev[a], and O. V. Glukhov[c]

[a] *Karazin Kharkiv National University, Kharkiv, 61000 Ukraine*

[b] *Bakul Institute for Superhard Materials, National Academy of Sciences of Ukraine, Kyiv, 04074 Ukraine*

[c] *National University of Radio Electronics, Kharkiv, 61166 Ukraine*

*****e-mail: atmu@meta.ua*

Received July 14, 2022; revised July 14, 2022; accepted July 20, 2022

Abstract—The phase composition, element distribution, and mechanical properties of the TiSiN/NbN(TiN) multilayer coatings obtained by vacuum arc deposition are anlyzed. The effect of the bias potential on the mechanical and tribological characteristics of the coatings is studied, and the adhesion strengths of the coatings to the substrate are measured. The results of X-ray diffraction studies of the coatings show that a two-fold increase in the bias potential leads to increases in all phase and structural parameters—in particular, lattice parameters, crystallite sizes, and microdeformation levels of the components of the coatings. The intensities of δ diffraction peaks of TiN and NbN indicate the presence of a strong (200) texture. Tribotechnical studies of the coatings have shown that they are erased during scratching, but their detachment from the substrate has not been recorded. This means that the coatings are worn by the cohesive mechanism associated with plastic deformation and the formation of fatigue cracks in the coating volume. Different modes of coating formation correspond to different values of acoustic emission that occurs, depending on the conditions, in the loading zone.

Keywords: vacuum–arc sputtering, multilayer coatings, bias potential, hardness, adhesive strength

DOI: 10.3103/S1063457622060041

INTRODUCTION

The development and application of new coating materials to improve the functional properties of the cutting tool (increasing the cutting speed, improving the quality of the machined surface, increasing the service life of the product, etc.) is among the most promising fields in the development of modern materials related to cutting processes. Refractory metal nitrides that are widely used in various industries exhibit high hardness, but they oxidize at a temperature of 550°C [1], which requires their further improvement. The processing methods, properties, and applications of titanium nitride (TiN) are the most systematically studied areas of transition metal nitrides. Titanium nitride crystallizes with the NaCl structure and exists as a solid solution containing nitrogen (from 37.5 to 50 at %). The structure and characteristics of coatings using TiN occurs improve due to the creation of multiphase compositions, such as the ternary, quaternary, and multicomponent ones. The currently used TiSiN ternary coating performs better than the TiN mononitride coating and so me ternary coatings, such as TiAlN, TiZrN, and TiVN [2]. The addition of silicon to TiN substantially improves its oxidation resistance and thermal stability. Moreover, the Ti–Si–N system even with a small concentration of element Si forms the *nc*-TiN/Si_3N_4 binary nanocomposite structure (the amorphous phase of Si_3N_4 surrounds the nanocrystalline phase of TiN), which directly improves its strength characteristics (hardness, crack resistance, wear resistance, etc.) [3].

In addition, the formation of a multilayer structure that contains nanoscale layers is an effective way to improve the properties of nanocomposite coatings. The proportion of interfaces in the structure of the coating material increases under such conditions, which makes it possible to simultaneously increase their hardness and viscosity. Among different binary transition metal nitrides, niobium nitride (NbN) is probably the best candidate, which can serve as a material of the second layer of the multilayer structure

Table 1. Technological parameters of deposition of the TiSiN/NbN coating

Sample	Current, A		Bias potential U_b, V	Working gas pressure p_N, Pa
	arc I_d	coil I_f		
A_1	110/80	0.5/0.5	−100	0.53
A_2			−200	
B_1			−100	0.05
B_2			−200	

together with TiSiN. Niobium nitride exhibits high hardness and corrosion resistance, and excellent chemical stability at high temperatures (1000°C), which will undoubtedly improve the stability and strength of the TiSiN composition. The coatings based on NbN are successfully used in industrial practice as a material for cutting tools and molds for pressure casting, which provides them with wear protection and corrosion resistance [4]. Recently, NbN exhibiting a high superconducting critical temperature and a high critical current density, as well as a low resistivity in the normal state, has been successfully used for the production of tunnel junctions, superconducting nanowire single-photon detectors (SNSPDs), hot electron bolometers (HEBs), etc.

In this regard, the development of protective coatings, one layer of which is a composite material, such as TiSiN, and the second one is a single-phase, such as NbN, is of considerable interest.

The aim of this study was to analyze the influence of deposition technological parameters—in particular, the bias potential and the working gas pressure—on the formation of multilayer nanostructured nitride coatings of the TiSiN/NbN systems and to investigate their properties.

EXPERIMENTAL

Multilayer coatings were formed by the method of vacuum arc deposition with use of two plasma sources by evaporation of TiSi and Nb cathodes in a nitrogen atmosphere during continuous rotation of the substrate with samples at a speed of 8 rpm. We used cathodes with the following chemical composition: TiSi with 94 at % Ti and 6 at % Si, and Nb of purity 98.2%. The substrate material was a plate made of 12Kh18N9T steel with a size of 20 × 20 × 3 mm.

The technological conditions for obtaining an experimental coating are given in Table 1.

Electron microscopy images of the cross section of the coating were obtained on a Novascan 450 scanning electron microscope, and its elemental composition was analyzed. The structure and phase composition of the coating were studied by X-ray diffraction in CuK_α radiation on a DRON-4 device. The microhardness values were determined using an HMV-G21ST ultramicrohardness meter from the Shimadzu company with a load on the indenter of 490.3 mN. Sclerometric tests were carried out using an REVETEST scratch tester under the following conditions: the load on the indenter was increased from 0.9 to 190 N, the load speed was 15.8 N/min, the speed of the indenter movement was 1 mm/min, and the scratch length was 12.0 mm.

RESULTS AND DISCUSSION

The chemical composition of the obtained coating is given in Table 2. The results show that there is a decrease in the concentration of silicon in the coating with an increase in the partial pressure of nitrogen to 0.53 Pa. Given that the mean energy of Ti ions is 122 eV (which is much higher than the average energy of Si ions (97 eV) [5]), this gives rise to the impoverishment of the plasma flow with less energetic particles during the collision of metal atoms with the gas flow. On the other hand, this process is facilitated by the selective sputtering of silicon in the flow of cathode particles, which is consistent with the published results [6] that the atomic content of the coating components differs from the ratio of their concentration in the cathode. The concentration ratio of light elements (silicon) is lower than their content in the cathode. According to [7], the concentration ratio of the components in the coating varies depending on the bias potential on the substrate, the working gas pressure in the chamber, and the presence or absence of a focusing field.

Figure 1 shows an electron microscopic image of a cross section of the TiSiN/NbN multilayer coating (sample B_2). As can be seen from Fig. 1, the coating applied to the steel substrate is uniformly distributed

Table 2. Chemical composition of the TiSiN/NbN coating

Sample	Elemental composition, at %			
	N	Ti	Si	Nb
A_1	21.59	35.81	1.52	41.07
A_2	24.33	35.57	1.37	38.73
B_1	10.45	38.87	1.90	48.78
B_2	18.47	41.23	1.42	38.68

and has a dense structure without pores, cracks, or other structural defects. A clear periodic arrangement of nanoscale layers in a multilayer architecture was observed. The thickness of the NbN layers is slightly greater (up to 20%) than that of the TiSiN layers. On the one hand, this phenomenon can be explanation by a lower evaporation rate of the TiSi cathode, which mainly consists of the refractory intermetallic compound $TiSi_2$ in contrast to the cathode made of high-purity NbN. On the other hand, the smaller thickness and higher density of TiSiN can be attributed to the lower energy of formation of the TiSiN compound compared to the NbN binary compound.

As was established from the results of X-ray diffraction analysis, the studied experimental coatings show different ratios of the (111) and (200) diffraction peaks, which depend on the value of the bias potential (−200 and −100 V) applied to the substrate. Thus, the X-ray diffraction pattern of the coating (Fig. 2), which is recorded with a bias potential of $U_b = -100$ V and a pressure of 0.53 Pa, revealed the two phases: cubic TiN in the first layer and cubic δ-NbN in the second layer. The lattice parameter of TiN is a = 0.4272 nm, and the size of the coherent scattering region (CSR) is D = 6.5 nm at the level of microstrains of $\varepsilon = 4.07 \times 10^{-3}$. The lattice parameter of δ-NbN is a = 0.4392 nm, and the CSR size is D = 6.9 nm at the level of microstrains of $\varepsilon = 5.77 \times 10^{-3}$. The distribution of line intensities of both of the phases indicates the presence of a strong (200) texture in TiN and δ-NbN.

The X-ray diffraction pattern of the coating recorded with $U_b = -200$ V and a pressure of 0.53 Pa revealed the two phases: cubic TiN and cubic δ-NbN. In addition, the X-ray diffraction pattern contains an additional line (at an angle of $2\theta = 47.97°$), which probably belongs to hexagonal δ'-NbN (the lattice parameters published in ICDD PDF-2 no. 65-3417 are a = 0.2968 nm and c = 0.5549 nm). The lattice parameter of TiN is a = 0.4312 nm, and the CSR size is D = 15.0 nm at the level of microstrains of $\varepsilon = 5.60 \times 10^{-3}$. The lattice parameter of δ-NbN is a = 0.4405 nm, and the CSR size is D = 18.2 nm at the level of microstrains of $\varepsilon = 5.85 \times 10^{-3}$. The intensity distribution of X-ray diffraction lines of TiN and δ-NbN indicates the presence of a strong (200) texture in these phases. The lattice parameters and substructural characteristics of hexagonal δ'-NbN could not be determined, since there is only one diffraction line of this phase.

Figure 3 shows fragments of X-ray diffraction patterns of the TiSiN/NbN coating synthesized with p_N = 0.05 Pa. As was established from the results of processing the received data, cubic nitride phase (Ti,Nb)N based on titanium and niobium nitrides is formed in these coatings. In sample B_1 obtained with a bias potential of $U_b = -100$ V, the lattice parameter of (Ti,Nb)N is a = 0.4351 nm and the CSR size is D = 6.3 nm at the level of microstrains of $\varepsilon = 1.82 \times 10^{-3}$. In sample B_2 obtained with a bias potential of

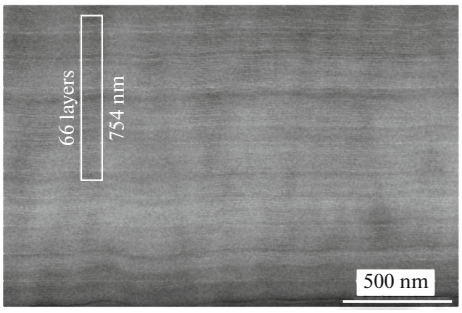

Fig. 1. Section of the TiSiN/NbN coating synthesized with $U_b = -200$ V and p_N = 0.53 Pa.

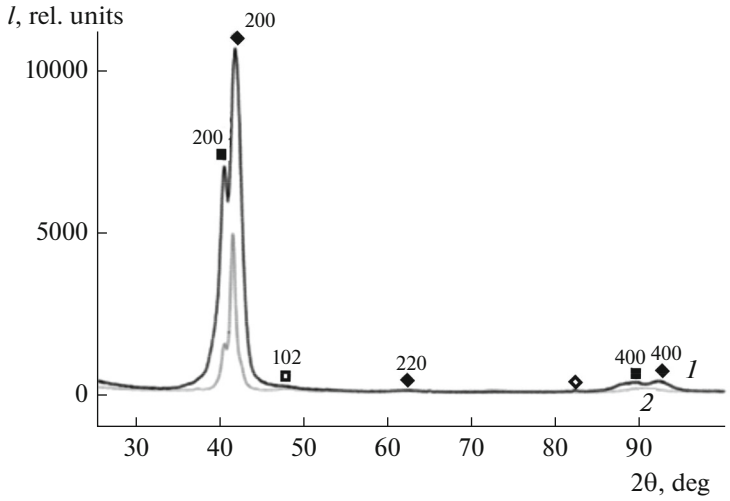

Fig. 2. Fragments of X-ray diffraction patterns of the TiSiN/NbN coating synthesized with p_N = 0.53 Pa for samples (*1*) A_1 and (*2*) A_2 comprised of (◆) TiN, (■) δ-NbN, (□) δ'-NbN, and (◇) a substrate.

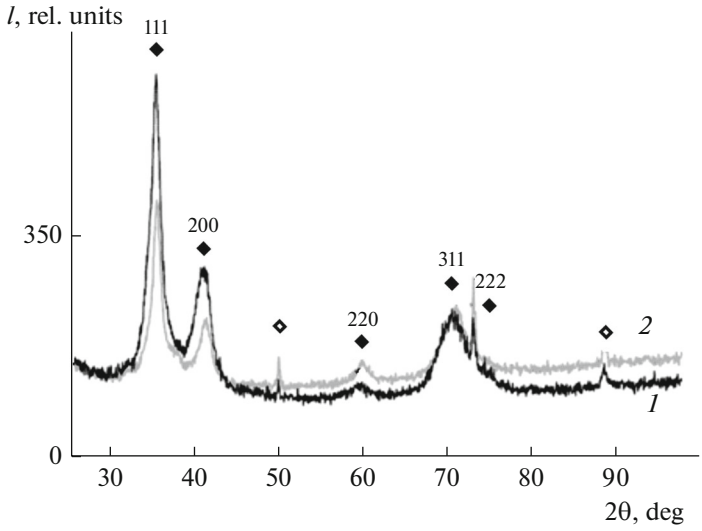

Fig. 3. Fragments of X-ray diffraction patterns of the TiSiN/NbN coating synthesized with p_N = 0.05 Pa for samples (*1*) B_1 and (*2*) B_2 comprised of (◆) (Ti,Nb)N and (◇) a substrate.

$U_b = -200$ V, only the cubic nitride phase based on titanium and niobium nitrides (Ti,Nb)N was detected, similarly to sample B_1, the lattice parameter of which is $a = 0.4335$ nm and the CSR size is $D = 6.3$ nm at the level of microstrains of $\varepsilon = 1.38 \times 10^{-3}$. The intensities of diffraction lines from the (111) and (311) planes is overestimated compared to the untextured state. That is, the texture in these coatings is complex (has several components), which is characterized by an intermediate state during the (200) → (111) transformation.

In general, the X-ray diffraction studies have shown that the phase composition of the TiSiN/NbN coating deposited under different deposition regimes varies greatly in the diffraction line shapes and intensities. The detected difference in the phase composition and the preferential growth direction of the coating indicates their substantial dependence on the working gas pressure and the bias potential, respectively.

Indentation is the most accurate method of determining the hardness and Young's modulus, which is theoretically and experimentally confirmed and standardized for studying the physical and mechanical properties of materials with a fine structure. The results of measuring the hardness of the TiSiN/NbN

Table 3. Mechanical properties of the TiSiN/NbN coating

Sample	Hardness H, GPa	Young modulus E, GPa	H/E	H^3/E^2
B_1	20.7	311	0.066	0.091
B_2	22.3	329	0.067	0.1
A_1	27.9	348	0.08	0.17
A_2	34.4	412	0.083	0.23

coatings are given in Table 3. It is obvious that the samples obtained with a high value of the working gas pressure (0.53 Pa) have the higher hardness (>27 GPa) and higher Young's modulus (>340 GPa). At the same time, an increase in the bias potential to −200 V leads to the formation of a coating with the best mechanical properties characterized by $H = 34.4$ GPa and $E = 412$ GPa. In particular, this is related to the phase composition of this sample, which has a complex nature, since the formation of a diffraction reflection that is probably attributable to hexagonal δ'-NbN was established in addition to reflections of the phases of cubic titanium nitride and niobium.

It is well known that the H/E^* (elastic strain of fracture) and H^3/E^{*2} (resistance to plastic deformation) ratios are important characteristics of functional coatings in addition to the hardness and induced Young's modulus values [8].

The calculated values of the H/E^* and H^3/E^{*2} ratios of the investigated multilayer coating samples indicate that a high H/E^* value (≥0.1) is associated with a decrease in the contact pressure, since the applied load is distributed over a large area. Therefore, such materials with high H/E^* values demonstrate high wear resistance and can be recommended for industrial applications [9, 10].

The increase in the hardness when switching to a multilayer architecture is associated with several additional effects. The most effective mechanism of blocking dislocations in multilayer systems is the Köhler effect. In a multilayer coating, extremely high shear stresses are required to move dislocations through the coating structure due to different shear moduli of the layers [11]. In the case of the TiSiN/NbN coating, the increase in the hardness is also caused by the formation of the nanosized NbN phase, which additionally hinders the movement of dislocations. In addition, the lattice mismatch between the crystalline layers of TiSiN and NbN effectively promotes strengthening due to alternating stress–strain fields caused by elastic coherence strains. The multilayered architecture contributes to the reduction of the grain sizes and the increase of the volume fraction of atoms located at the layer interfaces, thereby preventing the propagation of dislocations. This dependence is performed in the nanometer range of crystallite sizes (from ≥10 to 100 nm). It is assumed that grain boundary sliding or grain rotation occurs when grinding the grains below the critical size. This can explain the decrease in the hardness of the material with a very small grain size. Achieving a superhard state in nanostructured coatings is possible in the case of creating a structure with nanograins without dislocations or with a small number of them, and this factor is more important than the size of interatomic bonds in the crystal lattice [12]. As was established in [13], the sources of dislocation propagation cannot act in nanograins with sizes less than 10 nm, since such nanograins are free of dislocations, and the existing dislocations are not stable—for example, they are pushed into the amorphous matrix and disappear—and the amorphous matrix itself adapts to the crystal lattice mismatches of randomly oriented nanocrystallites. Taking into account the formation of the Si_3N_4 amorphous phase, the TiSiN/MeN multilayer coatings can have a nanocomposite structure and trigger the above-described strengthening mechanism.

The H/E^* parameter of the TiSiN/NbN multilayer coatings is higher than the H/E^* ratios of relatively soft single-layer Ti and TiN films (0.044 and 0.067, respectively [14]), which indicates their resistance to deformation and makes them promising for use as wear-resistant coatings.

The synthesized multilayer TiSiN/NbN coating (sample A_2) shows the highest H/E^* and H^3/E^{*2} parameters among all the investigated coatings. Separately, it is worth noting the substantially different value of resistance to plastic deformation (0.23). The H^3/E^{*2} ratio makes it possible to predict the mechanisms of localized deformation; inhomogeneous deformation (with the formation of shear steps) occurs only with low values of this parameter.

The adhesive strength is another important characteristic of coatings [15]. The scratch testing method was used to determine the adhesive strength. Samples A_1 and A_2 synthesized under the same nitrogen pressure ($p_N = 0.53$ Pa), but with different bias potentials U_b (−100 and −200 V, respectively) were tested (see Table 4).

Table 4. Results of adhesion tests of the TiSiN/NbN coating

Sample	Load *Lc*, N					Bias potential U_b, V
	Lc_1	Lc_2	Lc_3	Lc_4	Lc_5	
A_1	4.75	9.82	16.51	33.77	44.26	−100
A_2	15.02	27.3	30.42	43.99	49.76	−200

The coefficient of friction for different stages of wear, the amplitude of the acoustic emission, and the minimum (critical) load were determined as a result tests (load Lc_1 corresponds to the onset of penetration of the indenter into the coating, Lc_2 corresponds to the appearance of the first cracks, Lc_3 corresponds to the the appearance of clusters of cracks, Lc_4 characterizes the peeling of some regions of the coating, and Lc_5 characterizes the chipping of the coating or its plastic abrasion).

In the process of testing the coatings, it is possible to determine the limiting values of the critical failure load. According to the results of testing the coating synthesized with $U_b = -200$ V and $p_N = 0.53$ Pa (sample A_2), cohesive failure begins at a minimum load of $Lc_1 = 15.02$ N, and for the coating obtained with $U_b = -100$ V and $p_N = 0.53$ Pa (sample A_1), failure begins under a load of $Lc_1 = 4.75$ N (see Table 4 and Fig. 3). This result is indicative of the high cohesive strength of sample A_2. Under a load of $Lc_2 = 27.3$ N, slight peeling of the coating was observed at the edges of the scratches (see Fig. 4, sample A_2), which correlates with an increase in the intensity of the amplitude of acoustic emission (*AE*). The comparative analysis shows that TiSiN/NbN coating samples are worn during scratches, but not exfoliated, i.e., they are destroyed by a cohesive mechanism associated with plastic deformation and the formation of fatigue cracks in the coating material. They showed a high adhesive strength and a relatively low degree of delamination. The constant increase in the coefficient of friction with an increase in the load increases can be associated with the gradual degradation of the coating, which leads to the formation of wear products in the form of particles consisting of solid nitrides and leads to coating abrasion (Fig. 3, sample A_2).

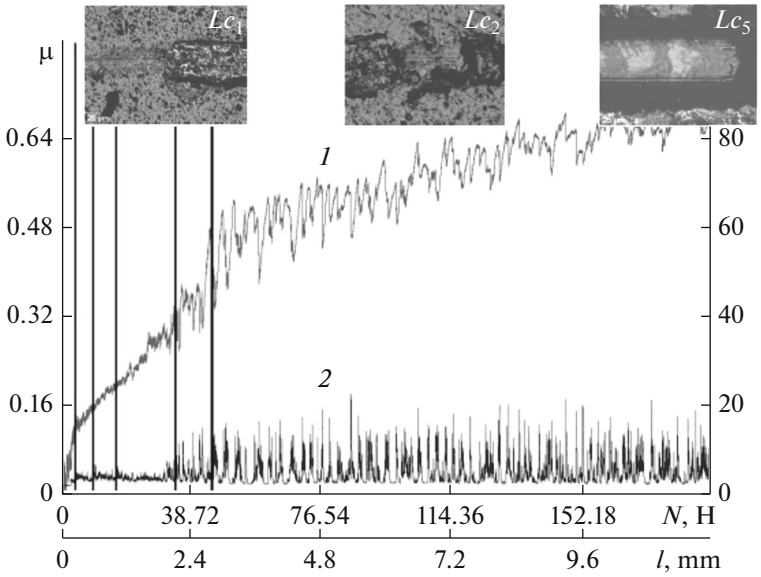

Fig. 4. The results of studying the properties of the TiSiN/NbN coating synthesized with $p_N = 0.53$ Pa and $U_b = -200$ V: (*1*) amplitude *AE*, %; (*2*) friction coefficient μ.

Similar results were obtained for the TiSiN/NbN coating formed with $U_b = -100$ V and $p_N = 0.53$ Pa. Different regimes of coating deposition used in the study correspond to different *AE* values depending on the loads.

CONCLUSIONS

As a result of studying the TiSiN/NbN multilayer coating synthesized by the vacuum arc deposition method in the mode of continuous rotation of the substrate, the effects of deposition parameters, such as the bias potential and the working gas pressure, on the structural phase composition, mechanical, and adhesive characteristics of the coating are determined. It is found that an increase in the bias potential from −100 to −200 V under a stable working gas pressure of 0.53 Pa leads to increases in the lattice parameters of TiN and δ-NbN, in the crystallite sizes, and the level of microstresses, as well as to the formation of a predominant texture growth in the (200) plane. A decrease in the pressure of the working gas to 0.05 Pa causes the formation of a cubic nitride phase based on titanium and niobium nitrides (Ti,Nb)N in the coating. The texture of such samples is complex (has several components) and is characterized by an intermediate state during the (200) → (111) transformation of crystallographic planes. The CSR size is about 6.3 nm, and the level of microstrains varies within $(1.82–1.38) \times 10^{-3}$.

The maximum values of mechanical parameters are obtained for the sample synthesized with a bias potential of −200 V and a working gas pressure of 0.53 Pa, which are as follows: hardness 34.4 GPa, Young's modulus 412 GPa, H/E^* ratio 0.083, and H^3/E^{*2} ratio 0.23.

Adhesion strength tests indicate a cohesive mechanism of coating failure, which is associated with plastic deformation and the formation of fatigue cracks in the material. The load leading to plastic abrasion of the sample is more than 44 N, which indicates a high degree of coating strength and high adhesive properties of the contact between the coating and the substrate.

FUNDING

This study was supported by the National Research Foundation of Ukraine (grant no. 2020.02/0234).

CONFLICT OF INTEREST

The authors declare that they have no conflicts of interest.

REFERENCES

1. Aksenov, I.I., Andreev, A.A., Belous, V.A., Strelnitsky, V.E., and Khoroshikh, V.M., *Vacuum Arc: Plasma Sources, Coating Deposition, Surface Modification*, Kyiv: Naukova Dumka, 2012.
2. Lytovchenko, S.V., Mazilin, B.A., Beresnev, V.M., Stolbovoy, V.M., Kovalyova, M.G., Kritsyna, E.V., Kolodiy, I.V., Glukhov, O.V., and Malikov, L.V., (TiZr)N/(TiSi)N maitilayer nanostructured coatings obtained by vacuum arc deposition, *J. Nano- Electron. Phys.*, 2018, vol. 10, no. 5, 05041.
3. Beresnev, V.M., Lytovchenko, S.V., Horokh, D.V., Mazilin, B.O., Stolbovoy, V.A., Kolodiy, I.N., Kolesnikov, D.A., Grudnitsky, V.V., Srebniuk, P.A., and Glukhov, O.V., Tribotechnical properties of (TiZr)N/(TiSi)N multilayer coatings with nanometer thickness, *J. Nano- Electron. Phys.*, 2019, vol. 11, no. 5, 05037.
4. Mamun, M.A., Farha, A.H., Er, A.O., Ufuktepe, Y., Gu, D., Elsayed-Ali, H.E., and Elmustafa, A.A., Nanomechanical properties of NbN films prepared by pulsed laser deposition using nanoindendation, *Appl. Surf. Sci.*, 2012, vol. 258, pp. 4308–4313.
5. Maksakova, O.V., Zhanyssov, S., Plotnikov, S.V., Konarski, P., Budzynski, P., Pogrebnjak, A.D., Beresnev, V.M., Mazilin, B.O., Makhmudov, N.A., and Kupchishin, A.I., Microstructure and tribomechanical properties of multilayer TiZrN/TiSiN composite coatings with nanoscale architecture by cathodic-arc evaporation, *J. Mater. Sci.*, 2021, vol. 56, pp. 5067–5081.
6. Yushkov, G.Yu., Anders, A., Oks, E.M., and Brown, I.G., Ion velocities in vacuum arc plasmas, *J. Appl. Phys.*, 2000, vol. 88, 5618.
7. Zhang, S., Wang, H.L., Ong, S.E., Sun, D., and Xuan, L.B., Hard yet tough nanocomposite coatings—Present status and future trends, *Plasma Processes Polym.*, 2007, vol. 4, pp. 219–228.
8. PalDey, S. and Deevi, S.C., Single layer and multilayer wear resistant coatings of (Ti,Al)N: A review, *Mater. Sci. Eng., A*, 2003, vol. 342, pp. 58–79.
9. Musil, J. and Jirout, M., Toughness of hard nanostructured ceramic thin films, *Surf. Coat. Technol.*, 2007, vol. 201, pp. 5148–5152.

10. Leyland, A. and Matthews, A., On the significance of the H/E ratio in wear control: a nanocomposite coating approach to optimised tribological behavior, *Wear*, 2000, vol. 246, nos. 1–2, pp. 1–11.
11. Yashar, P.C. and Sproul, W.D., Nanometer scale multilayered hard coatings, *Vacuum*, 1999, vol. 55, pp. 179–190.
12. Sheinman, E., Superhard coatings from nanocomposites. Review of foreign publications, *Met. Sci. Heat Treat.*, 2008, vol. 50, nos. 11–12, pp. 600–605.
13. Veprek, S. and Reiprich, S., A concept for the design of novel superhard coatings, *Thin Solid Films*, 1995, vol. 268, nos. 1–2, pp. 64–71.
14. Major, L., Morgiel, J., Major, B., Lackner, J.M., Waldhauser, W., Ebner, R., Nistor, L., and Van Tendeloo, G., Crystallographic aspects related to advanced tribological multilayers of Cr/CrN and Ti/TiN types produced by pulsed laser deposition (PLD), *Surf. Coat. Technol.*, 2006, vol. 200, pp. 6190–6195.
15. Ou, Y.X., Lin, J., Tong, S., Sproul, W.D., and Lei, M.K., Structure, adhesion and corrosion behavior of CrN/TiN superlattice coatings deposited by the combined deep oscillation magnetron sputtering and pulsed dc magnetron sputtering, *Surf. Coat. Technol.*, 2016, vol. 293, pp. 21–27.

Translated by O. Kadkin